Putting a spin on it: amyloid aggregation from oligomers to fibrils

Zurlo, E.

1 Introduction

Neurodegenerative diseases are a category of disorders that are characterized by a progressive degeneration of the structure and function of the neurons. As described in more details below, the most widely spread of such diseases are Alzheimer's disease and Parkinson's disease and they are expected to increase still further in the future due to the ageing of the population, causing large distress for society and a large burden for economy. Although treatments may help relieve some of the physical or mental symptoms associated with neurodegenerative diseases, there is currently no way to slow disease progression and no available treatments. Research on neurodegenerative diseases has considerably expanded over multiple scientific disciplines, however more progress is still needed.

This thesis focuses on amyloid proteins, a class of proteins that convert into amyloid fibrils. Such proteins are of high interest because they are related to many of the neurodegenerative diseases, such as Parkinson's disease (PD), type II diabetes, Huntington's disease and Alzheimer's disease (AD). Spin-label electron paramagnetic resonance (EPR) is the method we employed to study these complex systems. This chapter presents a brief introduction to this thesis. We describe the general structures of proteins, the intrinsically disordered proteins and their relation to neurodegenerative diseases. We explain the basis of the solid phase synthesis technique and give a general overview of EPR and the methods applied in this work.

1.1 Proteins and their properties

1.1.1 Structure of Proteins

Proteins are large biomolecules composed of one or more long chains of amino acid residues, and perform a vast array of functions within an organism. A linear chain of amino acid residues is referred as a polypeptide. Short polypeptides are commonly called peptides, while a protein contains at least one long polypeptide[1]. In most cases proteins adopt a specific three-dimensional structure that allows them to carry out their specific functions in the cells. Generally, this protein structure is organized from primary to quaternary levels (Figure 1.1).

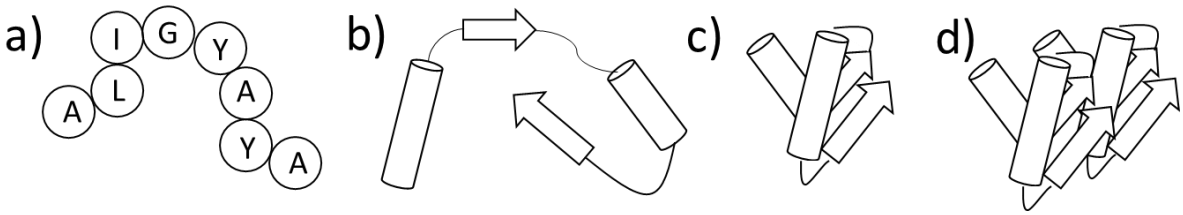

Figure 1.1 *Levels of protein structure. The primary amino acid sequence (a) (letters are acronyms of different amino acids) interacts to adopt secondary local structures (b). Compacting of these structures yields the global tertiary structure (c). Some proteins are active as quaternary complexes in which multiple polypeptide chains have associated (d).*

The order and number of the amino acids residues in the polypeptide chain is called the primary structure of a protein and contains all necessary information to adopt the final three dimensional structures of the protein[2]. The secondary structure of the protein is determined by hydrogen bonding between the amide and carbonyl groups of the protein backbone and is identified in different folding patterns, i.e. α-helices, β-sheets (Figures 1.1b, 1.2).

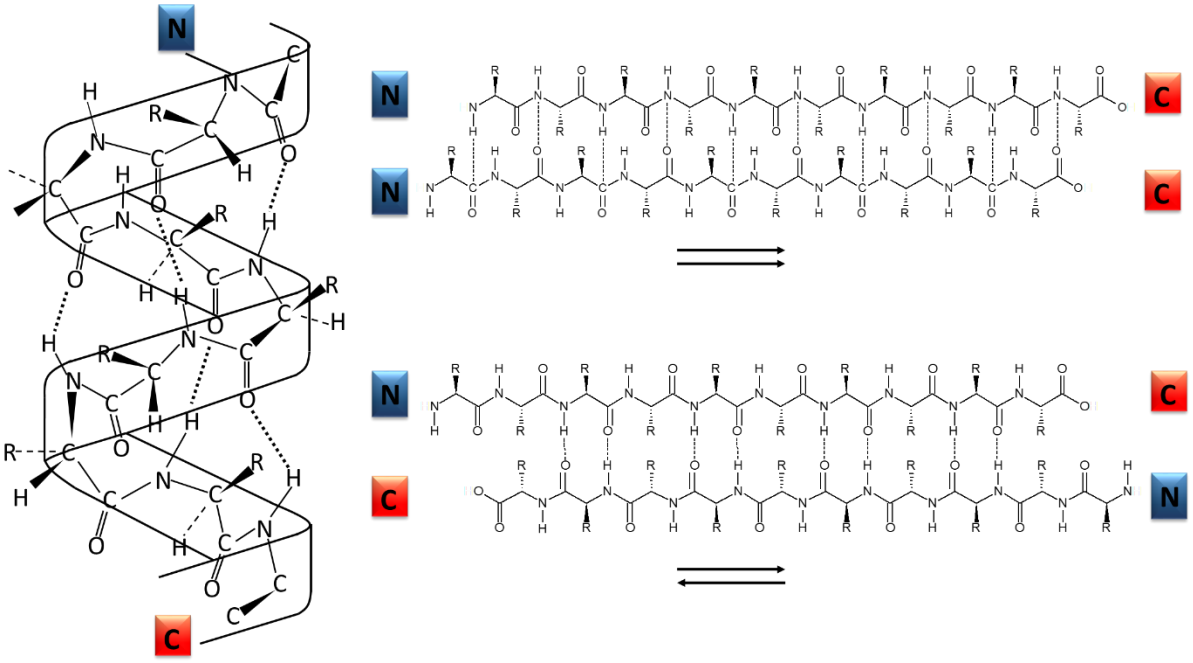

Figure 1.2 *Secondary structure elements of polypeptides. a) α-helix, b) parallel β-sheet, and c) anti-parallel β-sheet. The N and C in the boxes corresponds to the N-terminus and C-terminus respectively. The dotted lines represent the hydrogen bonds. Arrows show the direction of the β-strands in the β-sheet secondary structures.*

The typical α-helix is a right-handed helix with 3.6 amino-acid residues per turn and each turn has a pitch of 5.4 Å. The N-H group of an amino acid forms a hydrogen bond with the C=O group of the amino acid four residues earlier, as shown in Figure 1.2a. The β-sheet secondary structure, like α-helix, uses the full hydrogen-bonding capacity of its backbone, however, in this case, the bonds occur between neighboring polypeptide chains rather than a single chain. The direction of the chains categorize the β-sheet structure in two classes: Anti-parallel β-sheet and parallel β-sheet[3].

Further compacting of the secondary structures into the global conformation of the polypeptide chain forms the tertiary structure (Figure 1.1c). For most proteins, the tertiary structure is the final conformation adopted to become fully activated, however if proteins with a tertiary structure associate, a quaternary protein structure is formed (Figure 1.1d)[2].

1.1.2 Intrinsically disordered proteins

Proteins are considered to fold during their synthesis or immediately thereafter, and their function is assumed to be very closely related to their conformation. The structural characterization of the protein is considered key in understanding the biological role of these sequences. However, in the last few years, more and more of unstructured proteins have been discovered, and they are classified as intrinsically disordered proteins (IDPs)[4–6]. The IDPs are important components of the cellular signaling processes, allowing the same polypeptide to undertake different interactions with different consequences under different conditions[7,8]. Such IDPs can engage into non-functional intermolecular interactions and the proteins can aggregate into amorphous or amyloid-fibrils aggregates. Various IDPs without any sequence or conformational homology can form amyloid fibrils with similar characteristics[9]. This suggests that the main interactions within the fibril are made through the common protein backbone and not by the individual amino acid side chain residues, although these can influence the process. Amyloid fibrils are long, unbranched and often twisted structures with a diameter of 7-13 nanometers[9,10].

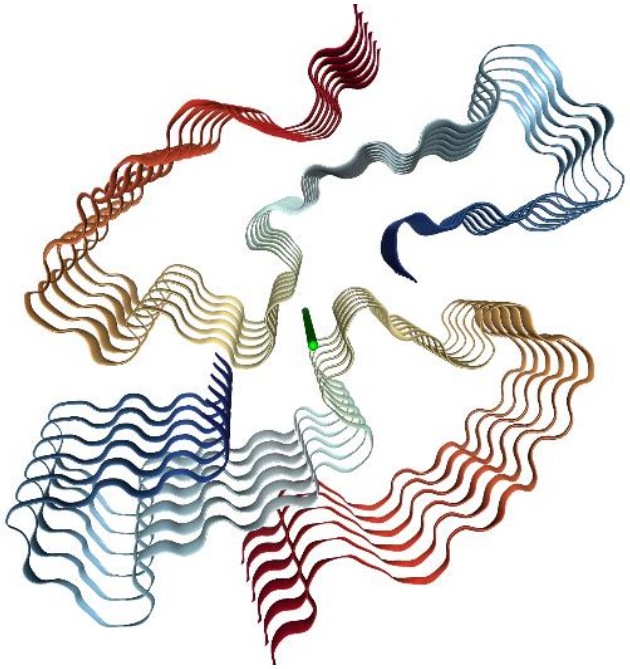

Figure 1.3 *Fibrillar structure of amyloid-β (42) obtained from Cryo-EM. The peptide chains are colored in rainbows to show directionality of amino acids sequences. In the center the fibril axis is shown.*[11,12]

Figure 1.3 shows that fibrils display typical cross-β structure. The proteins are structurally organized as β-strands oriented perpendicular to the fibril axis, with hydrogen bonds running parallel to the long axis of the fibril. Individual molecules are stacked every 4.7 Å along the axis; parallel, in register and stabilized by hydrogen bonding[12,13].

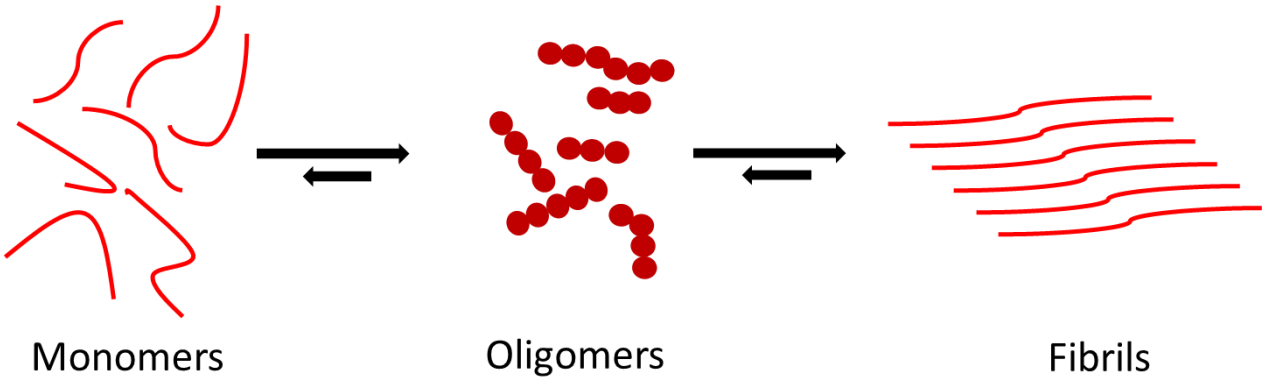

Figure 1.4 *Overall reaction pathway of amyloid aggregation shown schematically. Intrinsically disordered amyloid proteins in monomeric form (left), oligomer intermediates (shapes of oligomers are arbitrary), fibrils (right).*

The aggregation of IDPs to fibrils is considered to be a key aspect to understand the development of neurodegenerative diseases. The protein aggregation process is represented in a simplified way in Figure 1.4. Oligomers are intermediate species between the monomeric and fibrillary forms of the protein, and recent research seems to show that they are the toxic species implied possibly in the destruction of the cell membranes[14–20]. The oligomer formation is a rather obscure state in the amyloid aggregation process. It is still challenging to study the properties of such species due to their transient nature. In this thesis, Chapter 2,3 and 4 focus on the development and utility of new methods to study the properties of oligomers in amyloid systems.

1.1.3 Alzheimer's disease: the amyloid β peptide

Alzheimer's disease (AD) is the leading cause of dementia worldwide and more than 40 million people suffer AD. Clinically, AD is characterized by progressive cognitive impairment that inevitably leads to severe dementia, a stage marked by acute loss of almost all cognitive functions[21–24]. Biochemically and biophysically at the cellular level, AD is characterized by extracellular amyloid plaques and intraneuronal neurofibrillary tangles[22,25,26]. Amyloid plaques are extracellular deposits mainly build up from amyloid-β (Aβ) peptides. The Aβ peptide is the product of sequential proteolytic cleavage of the amyloid precursor protein, a transmembrane protein located in the neuronal membrane[27]. The predominant forms of Aβ contain 40 or 42 amino acids, commonly identified as Aβ40 and Aβ42, respectively. The Aβ42 is more hydrophobic, has a higher propensity to form insoluble fibrils, and thus, is more abundant in plaques than Aβ40,

however such properties make Aβ42 more difficult to study at the early stages of the aggregation process than Aβ40. In vitro toxicity studies have demonstrated that the Aβ assemblies are neurotoxic, but there is now general agreement that oligomers are the most pathogenic form of Aβ[28–31]. The potent pathological effects of the Aβ oligomers provide a compelling reason for the development of new methods to prevent their formation or to inhibit their activity. In Chapter 6 we study the effect of a potential drug inhibitor in the formation of Aβ aggregates.

1.1.4 Parkinson's disease: the alpha synuclein protein

Parkinson's disease (PD) is the second-most frequent neurodegenerative disorder, which affects primarily the population above 60 years of age[32]. The most obvious symptoms in Parkinson's disease include resting tremor, muscular rigidity, depression and difficulty with walking[33–35]. A cure to PD is difficult to develop, because the symptoms of the disease are difficult to detect at the early stage of the disease. Parkinson's disease is characterized by the accumulation of a neuronal protein, α-synuclein (αS), in Lewy bodies plaques in the brain, which are the pathological hallmark of Parkinson's disease. Misfolding and aggregation of the αS protein is accompanied by the loss of dopaminergic neurons in the *substantia nigra*, a region in the midbrain[36]. The αS protein (40 kDa) consists of 140 amino-acid residues and is part of the IDP class[4,5]. The function of the α-synuclein protein (αS) is associated with its ability to bind to the membranes of intracellular vesicles and thought to involve membrane remodeling and vesicle trafficking. It mainly localizes at the synaptic terminus where it plays a role in synaptic transmission[37]. Under certain conditions in vitro (see Chapter 4 of this thesis), αS forms oligomers and ultimately fibrils. Several works have shown that these oligomeric species are toxic to cells, and are related to the development of Parkinson's disease[38,39]. In Chapter 4 we investigate the aggregation kinetics of αS from monomers to fibrils using EPR to observe the formation of oligomers in situ.

1.1.5 Solid Phase Peptide Synthesis

Solid phase peptide synthesis (SPPS) was invented by Merrifield in 1963 and it has become widely used in peptide synthesis[40]. Small solid resin beads, insoluble yet porous, are treated with functional linkers onto which peptide chains can be built. The peptide remains covalently attached to the bead until cleaved. The peptide is thus immobilized on the solid-phase and can be retained during a filtration process, whereas liquid-phase reagents and by-products of synthesis are flushed away as shown in detail in Figure 1.5.

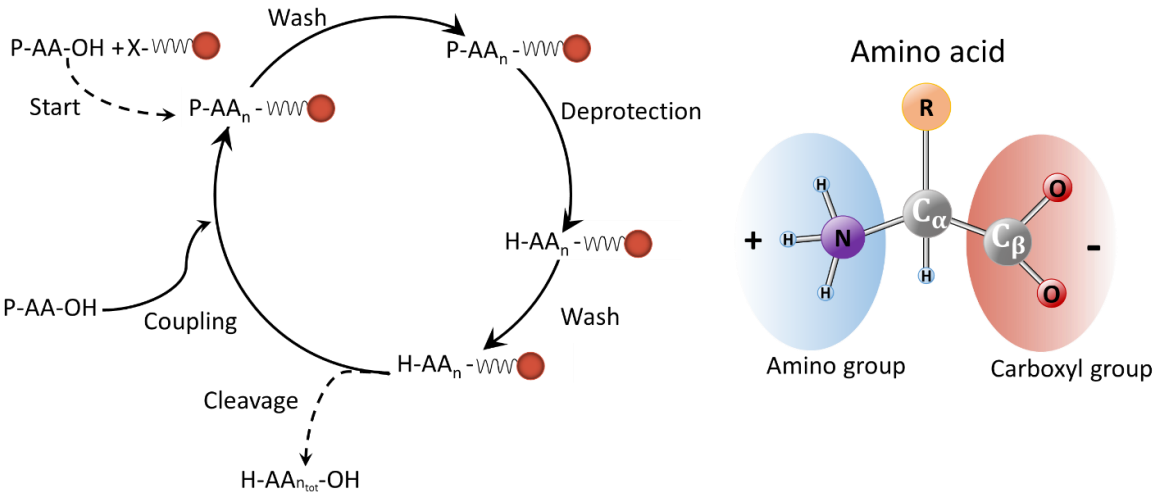

Figure 1.5 *The general process for synthesizing peptides on a resin. Start: The first amino acid (AA_n, n = 1), the C-terminal residue, gets attached to the resin though a linker. To prevent the polymerization of the amino acid, the amino group and the reactive side chains are protected with a temporary protecting group. Once the amino acid is attached to the resin, the resin is filtered and washed to remove byproducts and excess reagents. Next, the amino group protection is removed in a deprotection process and the resin is again washed to remove byproducts and excess reagents. Then the next amino acid is coupled to the attached amino acid (n + 1), usually with the addition of activation reagents of the carboxyl group. This is followed by another washing procedure, which leaves the resin-peptide ready for the next coupling cycle. The cycle is repeated until the peptide sequence is complete ($n = n_{tot}$). Then typically, all the protecting groups are removed and the peptide resin is washed, and the peptide is cleaved from the resin.*

The coupling reactions can be driven to completion and high yields through the use of excess reagent. In this method, the amino acids are protected at all reactive functional groups. The order of functional group reactions can be controlled by the order of deprotection. To take note is that unnatural amino acids can be added to the sequence, as shown in Chapters 2, 3 and 6 of this thesis. Another main advantage of SPPS is the increased simplicity and speed of the entire process compared to in-solution synthesis.

1.2 Electron paramagnetic resonance

Electron paramagnetic resonance (EPR) is a powerful spectroscopic technique useful to study systems with at least one unpaired electron (paramagnetic species) such as organic and inorganic free radicals or transition metal ion complexes. Stable radicals like nitroxide radicals are widely used as spin probes in biological samples.

The EPR technique is a magnetic resonance spectroscopy, relying on the same concepts as NMR. The splitting of the electron-spin energy levels (Figure 1.6) is due to the presence of an external magnetic field (B_0). The transitions between the energy levels can be induced by on-resonant microwave radiation. Two main categories of EPR experiments can be distinguished: continuous-wave (cw) experiments and pulsed EPR measurements. The extensive development of EPR techniques is providing new possibilities to get insights into the nature of the paramagnetic species and their surroundings. Here will be

given a brief overview of the basic principles of EPR. More details can be found for example in the monographies of Atherton and Brustolon[41–43].

1.2.1 Electron Zeeman interaction and g-factor

When an electron is subject to an external magnetic field, the energy levels associated with its spin split up as a function of the magnetic field, see Figure 1.6. The quantum mechanical description of this phenomenon is given by the spin Hamiltonian ($\mathcal{H}$) in eqn. (1.1):

$$\mathcal{H} = g_e \mu_B \boldsymbol{S} \cdot \boldsymbol{B} \tag{1.1}$$

where $g_e = 2.0023$ is the g-factor of an isolated electron in vacuum, μ_B is the Bohr magneton, **B** is the external magnetic field, and **S** is the electron spin operator. The magnetic field is oriented along one direction, conventionally *z*, so only the magnetic field B_0 along that axis is taken into account, and therefore only the S_z component in the spin operator **S** is considered. For a system that contains an electron spin $S = ½$, the eigenvalues of S_z are $m_s = \pm\frac{1}{2}$, thus equation 1.1 can be rewritten as:

$$E_{\pm} = \pm\frac{1}{2} g_e \mu_B B_0 \tag{1.2}$$

which evidences the linear dependence of the splitting of the energy levels from the strength of the external magnetic field (B_0), shown in Figure 1.6.

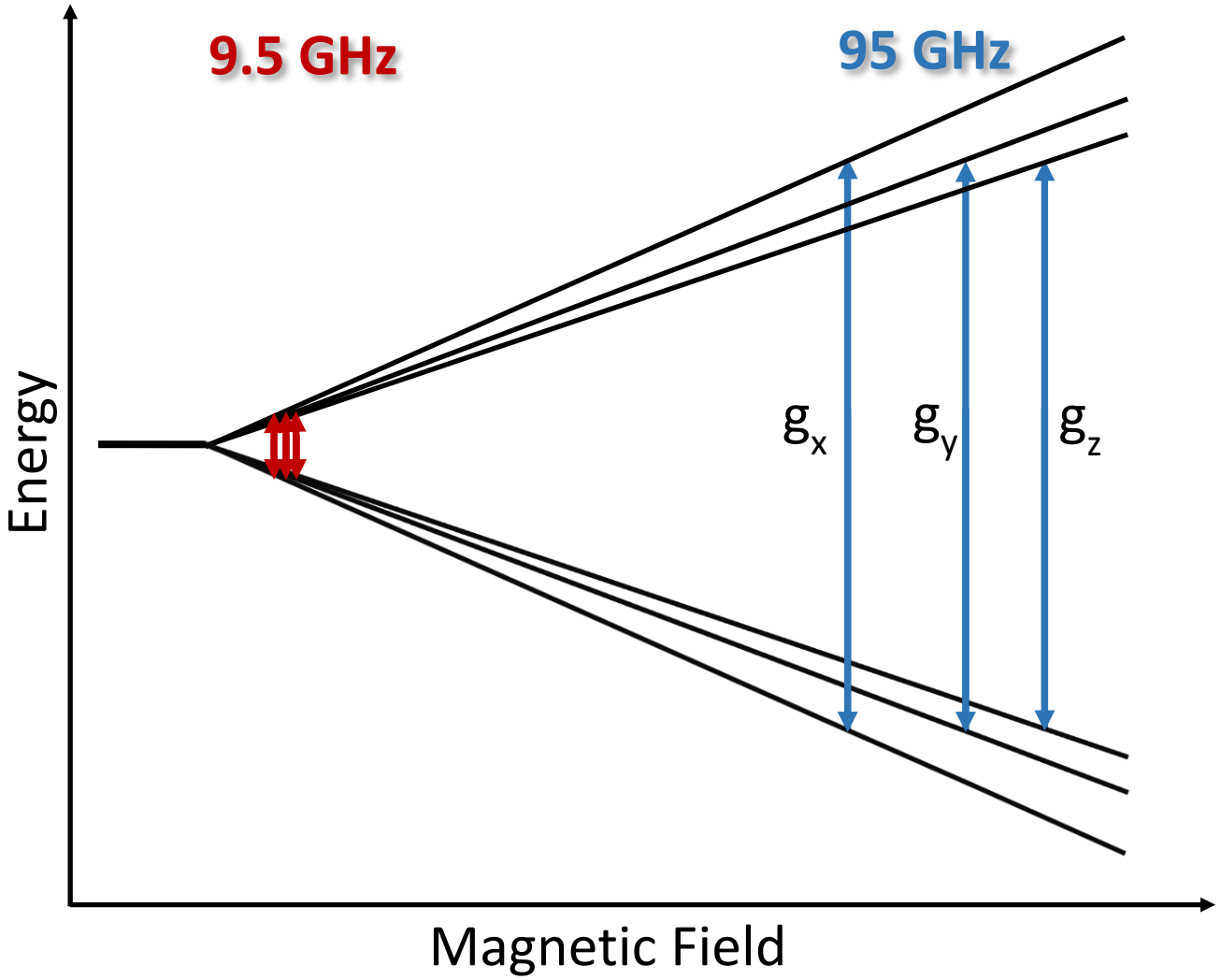

Figure 1.6 *Schematic representation of the electron spin energy levels (black lines) for a S = ½ system with anisotropic* ***g*** *subjected to the Zeeman effect in the presence of an external magnetic field (B_0). The red arrows and blue arrows represent the EPR transitions at lower and higher frequencies, respectively.*

The splitting of the energy levels is proportional to the g-factor, a variable that is sensitive to the electronic properties of the molecule or ion the unpaired electron is part of, comporting a variation from g_e. The **g** is a tensor and as such is anisotropic: The splitting of the energy levels depends on the orientation of the molecule or ion relative to the magnetic field direction. Figure 1.6 shows the splitting of the energy levels for an S = ½ system with an anisotropic **g** tensor as a function of the magnetic field. At higher magnetic field the anisotropy of the **g** tensor results in a larger separation of the transitions (arrows in Figure 1.6). This is an advantage of high-field EPR/high-frequency EPR compared to low-field EPR: In case of a small anisotropy of the **g** tensor, only high-field EPR enables to resolve the transitions.

1.2.2 Electron spin – nuclear spin interaction: hyperfine interaction

The interaction between nuclear spin(s) and the applied magnetic field is analogous to the electron Zeeman (EZ) interaction, however its magnitude is only 1/658 of the EZ interaction due the fact that the magnetic moment of a nuclear spin is much lower than the magnetic moment of an electron spin. In addition to the Zeeman interactions, one important aspect about spins is that they can interact with each other. The interaction between the magnetic dipoles of unpaired electrons and surrounding nuclei is called *hyperfine interaction,* and it is an important source of chemical information in EPR. The resulting spin Hamiltonian can be expressed as:

$$\mathcal{H} = g_e \mu_B \boldsymbol{S} \cdot \boldsymbol{B} - g_N \mu_N \boldsymbol{I} \cdot \boldsymbol{B} + \boldsymbol{S} \cdot \boldsymbol{A} \cdot \boldsymbol{I} \qquad (1.3)$$

where g_N represents the nuclear g-factor and μ_N is the nuclear magneton. The hyperfine interaction is given by the tensor **A** that consists of two contributions: The isotropic part and the anisotropic part, namely $\mathbf{A} = A_{iso} + \mathbf{T}$.

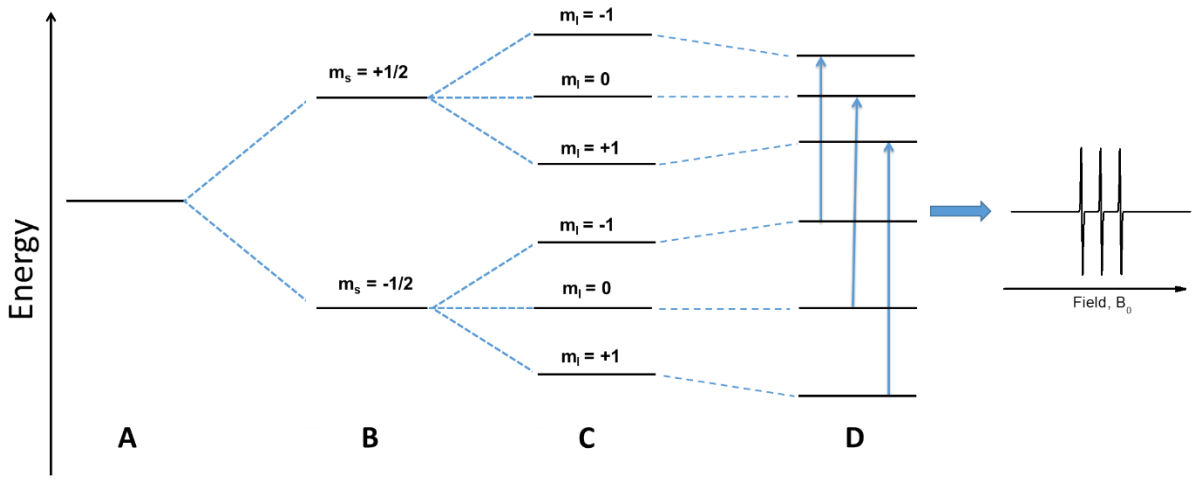

Figure 1.7 *Schematic energy levels representing the effects of the spin Hamiltonian of eq.1.3 for an electron with spin S = ½ and its interaction with a nuclear spin I = 1. (A) When there is no external magnetic field the spin states m_s = ½ and m_s = -½ are degenerate. (B) In the presence of an external magnetic field, the electron Zeeman interaction separates the energy levels of the two spin states. The g-factor is considered isotropic. (C) Another splitting of the energy levels is caused by the nuclear Zeeman interaction, which creates a separation of the energy levels of the nuclear spin states m_I = -1, m_I = +1 and m_I = 0. (D) The hyperfine interaction between the electron spin and nuclear spin (considered isotropic) causes another shift of the energy levels by an isotropic A_{iso}. The possible three transitions are shown by arrows, and the resulting EPR spectrum is shown on the right*.

Figure 1.7 shows the corresponding energy level scheme for a nitroxide radical, which contains an electron spin (S = ½) and a nitrogen nuclear spin ($^{14}N, I = 1$). The splitting of the energy levels is due to the electron Zeeman (EZ) interaction (Figure 1.7B), also the nuclear spin splitting (NZ) must be taken into account, so that each of the energy levels are further split according to the magnetic quantum numbers of the nuclear spin. As a last step, Figure 1.7D shows how the hyperfine interaction terms applies on the formed sublevels, shifting them by an amount defined by the hyperfine tensor **A**.

For anisotropic **g** and **A** tensors, the orientation of the magnetic field with respect to the molecular system or ion must be taken into account. The **g** tensor is characterized by three principal values, g_{xx}, g_{yy}, and g_{zz}, each corresponding to a particular orientation of the molecule in the magnetic field B_0 as shown in Figure 1.8 for a nitroxide radical. The principal values of the tensor **A** are A_{xx}, A_{yy} and A_{zz}. For nitroxide spin labels the difference between A_{xx} and A_{yy} is small and the hyperfine tensor can be considered to be axially symmetric. The value of A_{zz} is highly sensitive to the polarity of the environment and can give precious information about the surroundings of the spin label[44].

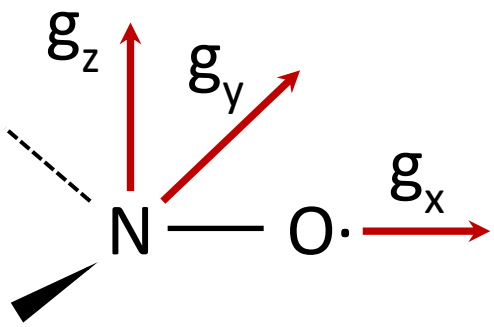

Figure 1.8 *Structure of a nitroxide radical. The unpaired electron (black dot) localizes on the N-O bond. Principal directions of the* ***g*** *tensor are shown (red arrows).*

1.2.3 Spin-label EPR

Spin labels are paramagnetic probes that can be attached to systems that do not contain a paramagnetic center. In nature, most bio-macromolecules do not contain paramagnetic centers, therefore they are EPR silent. With the development of site-directed spin labeling[45–47], EPR has become a powerful technique to investigate local structure and dynamics of proteins, to map distances between amino acid residues in polypeptides, and to understand the three-dimensional structure of bio-macromolecular complexes.

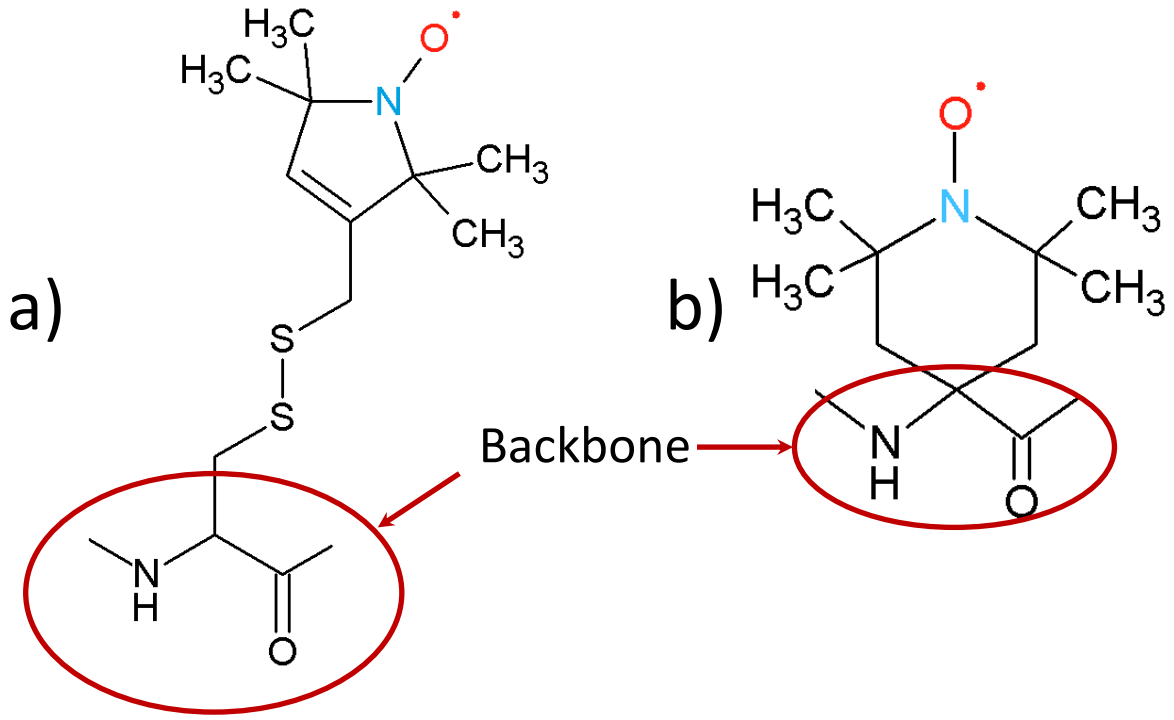

Figure 1.9 *a) Molecular structure of the MTSL spin label attached to a cysteine side-chain. b) Molecular structure of the TOAC spin label. The backbone of the peptide is shown as well.*

The most commonly used spin labels are nitroxide derivatives with a stable unpaired electron. The stability of the nitroxide radical is mostly given by the steric effect of the methyl groups adjacent to the nitroxide. Figure 1.9 shows the structure of the two nitroxide spin labels used in the research described in this thesis: the MTSL spin label [(1-oxyl-2,2,5,5-tetramethylpyrroline-3-methyl)-methanethiosulfonate], and the TOAC spin label (2,2,6,6-tetramethyl-N-oxyl-4-amino-4-carboxylic acid). The MTSL spin label attaches to a protein by a covalent bond between the –SH group of the cysteine and the methanethiosulfonate of MTSL, whereas the TOAC spin label is placed directly into the backbone of the protein.

1.2.4 Spin-label dynamics: The rotational correlation time

The cw-EPR in solution experiments on nitroxides are sensitive to the mobility of the label with respect to the external magnetic field, which gives rise to changes in the shape of the EPR spectrum. Any dynamic process on the timescale determined by the **g** and **A** tensor anisotropy affects the shape of the lines, giving information related to the structure and mobility of the protein[45–47]. The rotational motion of the paramagnetic species is characterized by the *rotational correlation time* (τ_r), which is the average time it takes for a molecule to rotate one radian, i.e. the longer τ_r the lower is the mobility of the nitroxide.

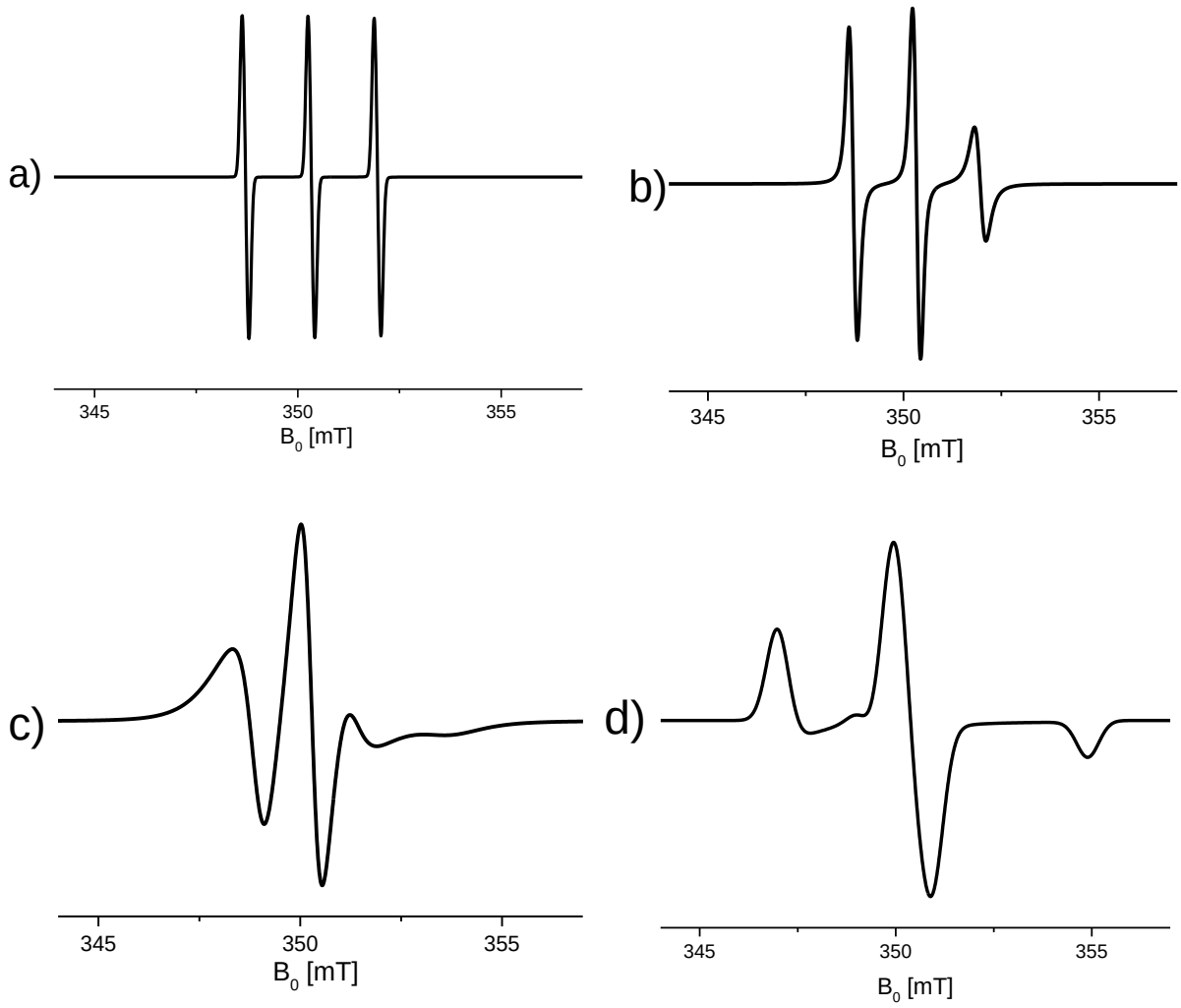

Figure 1.10 *Simulated cw-EPR spectra to show the effect of the rotational correlation time of a nitroxide spin label on the lineshape of the spectra. a) τ_r = 0.003 ns, b) τ_r = 0.5 ns, c) τ_r = 3.16 ns and d) frozen solution. The spectra a) and b) were simulated with the algorithm "garlic", c) with the algorithm "chili" and d) with the algorithm "pepper" using EasySpin[48]. The* ***g*** *tensor is [2.0086 2.0059 2.0020], and the hyperfine tensor is [13 13 110.7] MHz. The linewidth parameter for a), b), c) spectra is 0.12 mT, and for spectrum d) is 0.65 mT.*

Figure 1.10 shows the effect of the mobility of the spin label on the lineshape of the EPR spectra by a set of simulations. If the radical is completely free to move in solution the EPR spectrum has three narrow lines as shown in Figure 1.10a. The lines are spaced by the isotropic nitrogen hyperfine interaction (A_{iso}, see subsection 1.2.2), which is due to the hyperfine interaction of the unpaired electron ($S = ½$) with the ^{14}N nuclear spin ($I = 1$). With increasing τ_r the linewidth and intensity starts to vary: The slower the motion ($1 < \tau_r < 10$ ns), the broader the lines become, and the less intense the high field and low field lines appear (Figure 1.10 b,c). In the slow-motion regime the lines start to change position. For slow motion ($\tau_r > 10$ ns), the spectrum approaches that of a completely immobilized spin label and the anisotropy is fully observable (Figure 1.10d). In Chapters 2,3,4 and 6 of this thesis, we have used the lineshape changes in nitroxide-spin-label spectra to identify the formation and structure of amyloid systems.

1.2.5 Distance determination by EPR: Dipole-dipole interaction

An important part of modern EPR is the structure determination of biological systems, which is based upon the measurement of the distances between spin-labels. Such distances are derived from the dipole-dipole interaction between the unpaired electrons of the spin-labels. The dipole-dipole interaction (ν_{dd} in MHz units) between two spins, A and B, is inversely proportional to the cube of the distance and is given by:

$$\upsilon_{dd} = -\frac{\mu_0 \hbar}{8\pi^2}\frac{g_A g_B}{r_{AB}^3}(3cos^2\theta - 1) \qquad (1.4)$$

where μ_0 is the magnetic permeability in vacuum, g_A and g_B are the isotropic g factors of the two spins A and B, $\hbar$ is the reduced Planck's constant, r_{AB} is the distance between the two spins, and θ is the angle between the magnetic field and the vector that connects the two spins.

1.2.6 Double electron-electron resonance

The double electron-electron resonance (DEER) technique, also called pulsed electron double resonance (PELDOR), is a method to measure the dipole-dipole interaction between unpaired electrons for distances larger than 2 nm (Figure 1.11a). This technique allows the detection of the modulation of the echo intensity, which is caused by the dipole-dipole interaction between spins.[49]

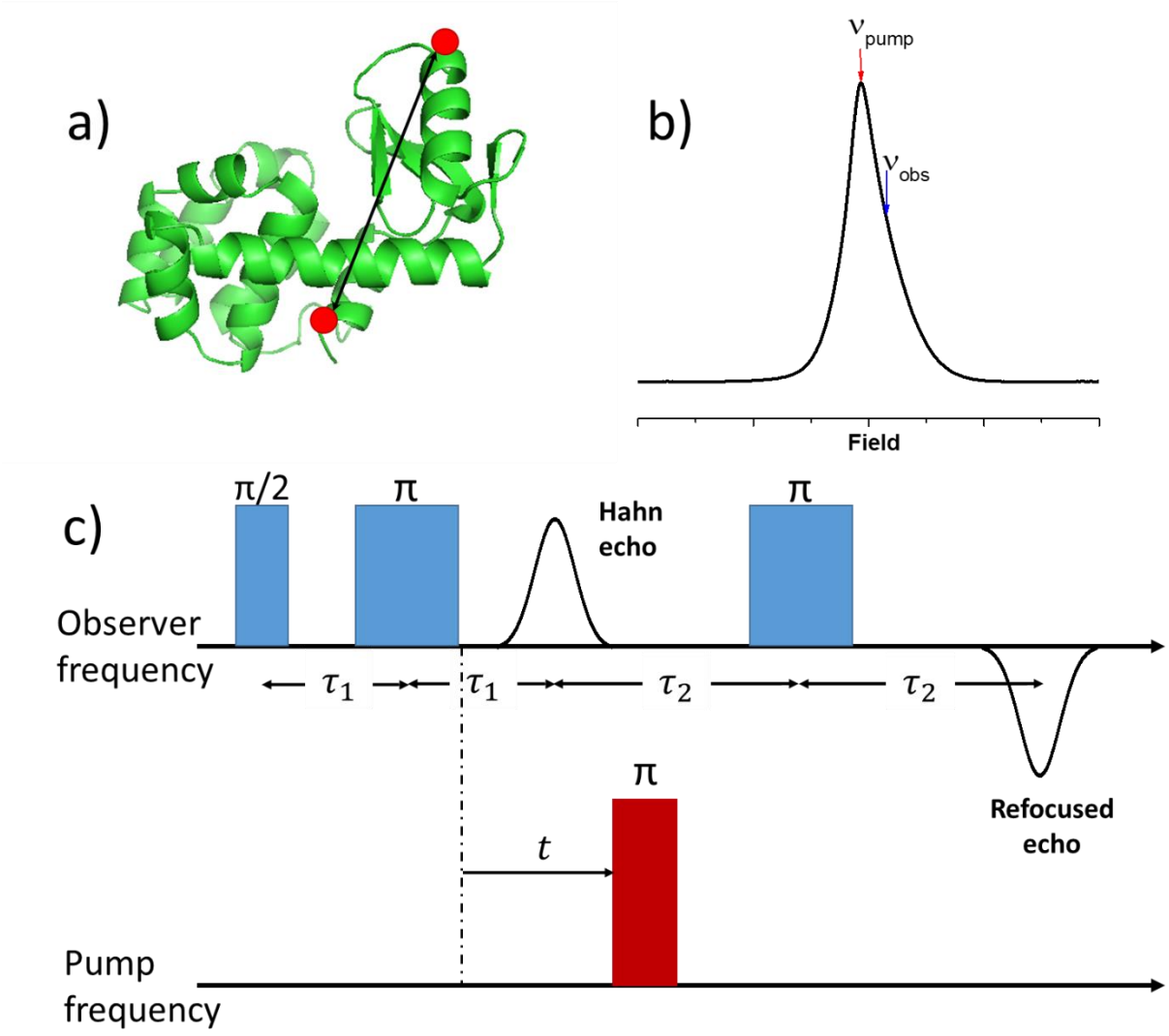

Figure 1.11 *Schematic representation of double electron-electron resonance (DEER) spectroscopy. A) Protein with two spin labels A and B (red dots). b) Field swept Hahn echo of a Gd(III) spin tag. Arrows show the frequency positions for the observer and pump pulses. c) Pulse sequence of the DEER experiment consisting of the refocused echo sequence at the observer frequency (ν_{obs}) and the pump pulse at the pump frequency (ν_{pump}). The delay times τ_1 and τ_2 are fixed. The delay time t varies and we follow the variation of the amplitude of the refocused echo in function of t.*

The pulse sequence of a standard DEER experiment is shown in Figure 1.11c. Two different microwave frequencies are applied (Figure 1.11b), the so-called pump and observer frequencies. At the observer frequency three pulses are employed to selectively monitor a refocused echo of one of the paramagnetic centers (A). The π/2 and π pulses rotate the magnetization of the spins by 90^0 and 180^0 respectively, resulting in a refocused echo (Figure 1.11c). An additional inversion pump pulse (π) between the second and third pulse at the observer frequency is applied with a frequency resonant with the second paramagnetic center (B) that selectively flips the spin B. This stimulated spin-flip induces a sudden change in the precession rate of the magnetization of spin A which leads to a nonperfect refocusing of the A spins, as a function of the dipolar coupling

between spins A and spins B (ν_{dd}). By variation of the time at which the inversion pulse is applied, the dephasing of the magnetization of spin A is changed to induce a periodic modulation of the A-spin refocused echo intensity, which is called the DEER time trace (Figure 1.12a). Applying the Fourier Transformation to the DEER trace, a Pake Pattern is obtained from which the dipolar coupling frequency (ν_{dd}) can be extracted as shown in Figure 1.12b.

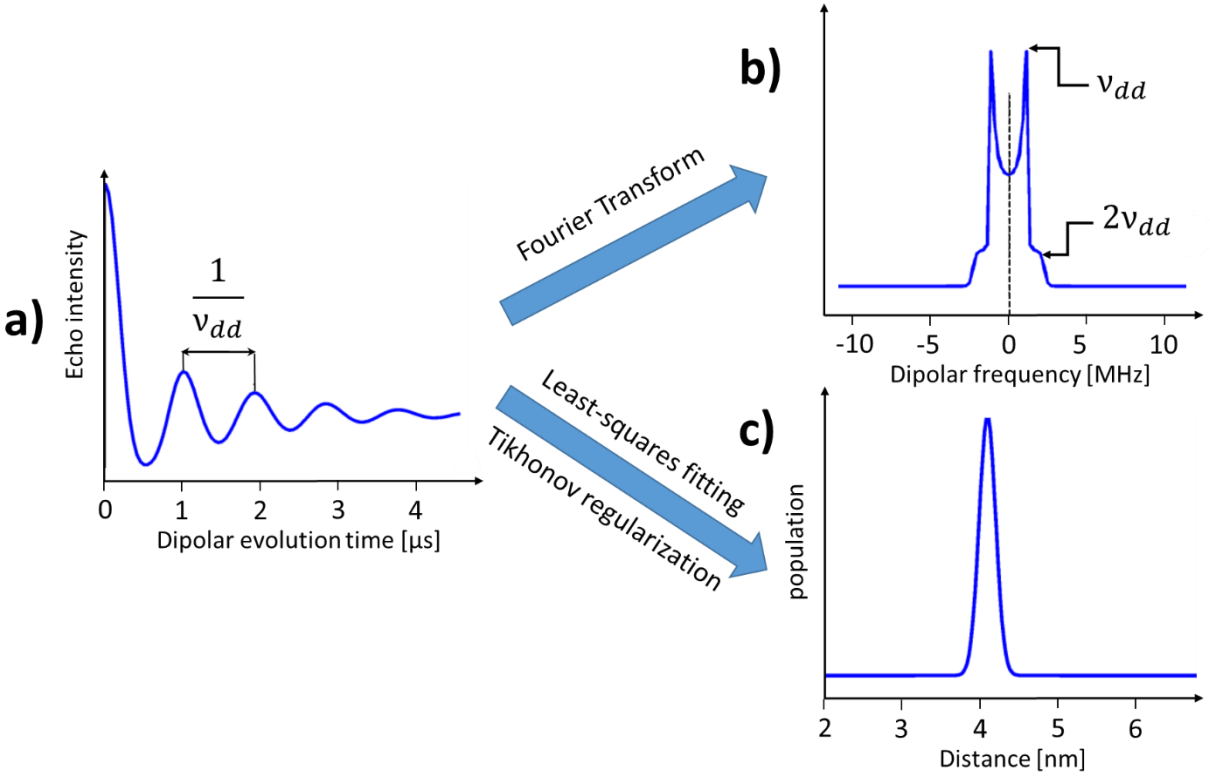

Figure 1.12 *Data analysis of a DEER trace. a) Model of a DEER trace with dipolar coupling modulation after background correction. b) Fourier transformation (Pake Pattern) of the DEER trace with peaks at ± ν_{dd} and edges at ± 2ν_{dd}. c) Distance distribution obtained by Tikhonov regularization.*

Due to the flexibility of the macromolecules and conformational freedom of the spin label, the distance between spins varies in a certain range. In the case of proteins often broad distance distributions result. The overall signal of a DEER trace shows the superposition of modulations at different frequencies, rather than a single frequency. Other approaches for the analysis are regularization methods or model-based approaches, by which the distance distributions are directly fitted to the DEER time traces (Figure 1.12c)[50–53]. In this thesis we used the Tikhonov regularization approach.

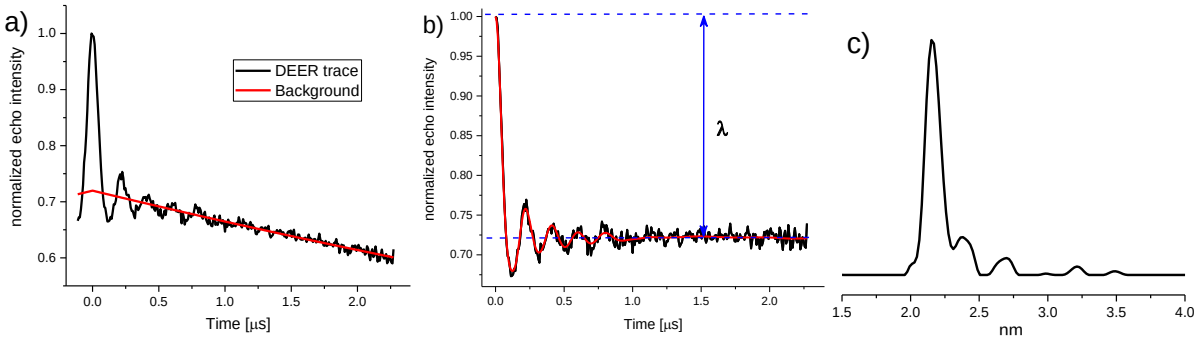

Figure 1.13 *Analysis steps of DEER time traces on a rigid doubly labeled system. a) Raw DEER time trace. Red line: Background fit. b) Background corrected DEER time trace. Red: Fitting of the modulation. Blue arrow: modulation depth (λ). c) Distance distribution obtained by Tikhonov regularization method*[54]*. Small features are probably artifacts.*

To determine the distance distribution between the two paramagnetic centers within the same molecule, the effects of the interaction of the spins within the same molecule must be separated from the contribution of the intermolecular interaction of the spins (background). The subtraction of the background is shown in (Figure 1.13b). The amount of coupled spins compared to the total echo intensity is given by the modulation depth (λ), as shown in Figure 1.13b. The spin-spin distance obtained from the analysis of the DEER trace, shown in Figure 1.13c, represents the distribution of the distances between the paramagnetic centers obtained by Tikhonov regularization. The width of such distribution is directly related both to the flexibility of the labeled macromolecules and to the conformational freedom of the paramagnetic centers[55,56].

1.3 Thesis outline

In Chapters 2 and 3, continuous wave (cw) EPR is employed to investigate the influence of the backbone attached TOAC spin labels on the aggregation of the amyloid peptides and its possible uses to study the structure and properties of amyloid oligomers. In Chapter 4, we examine the kinetics of aggregation of the spin-labeled αS protein by continuous wave (cw) EPR. In Chapter 5 we investigate with pulsed EPR the properties of three recently developed Gd(III) labeling tags. In the final Chapter we present the EPR characterization on how TOAC influences the aggregation of Aβ, and we apply it to investigate the effects of a recently discovered inhibitor of Aβ aggregation.